

# Scalar and tensor gauge field localization on deformed thick branes

W. T. Cruz,<sup>a,b</sup> M. O. Tahim,<sup>a,c</sup> and C. A. S. Almeida<sup>a</sup>

<sup>a</sup>*Departamento de Física - Universidade Federal do Ceará  
C.P. 6030, 60455-760 Fortaleza-Ceará-Brazil*

<sup>b</sup>*Centro Federal de Educação Tecnológica do Ceará (CEFETCE),  
Unidade Descentralizada de Juazeiro do Norte, 63040-000 Juazeiro do Norte-Ceará-Brazil and*

<sup>c</sup>*Departamento de Ciências da Natureza, Faculdade de Ciências,  
Educação e Letras do Sertão Central (FECLESC),  
Universidade Estadual do Ceará, 63900-000 Quixadá-Ceará-Brazil*

We make an analysis about several aspects of localization of a scalar field and a Kalb-Ramond gauge field in a specific four dimensional AdS membrane embedded in a five dimensional space-time. The membrane is generated from a deformation of the  $\lambda\phi^4$  potential and belongs to a new class of defect solutions. The study of deformed defects is important because they contain internal structures and these may have implications to the way the background space-time is constructed and the way its curvature behaves. The main objective is to observe the contributions of the deformation procedure to the well known field localization methods.

PACS numbers: 11.27.+d, 11.15.-q, 11.10.Kk, 04.50.-h

Keywords: Field theories in higher dimensions, Randall-Sundrum scenario, Kalb-Ramond field, Defect solutions

## I. INTRODUCTION

In a scenario of extra dimensions the observable universe is represented by a four-dimensional membrane embedded in a higher dimensional space-time. The standard model of particles is confined in the membrane while gravitation is free to propagate into the extra dimension. These ideas have appeared as alternatives to solve the gauge hierarchy problem [1]. Recently a lot of attention has been given to the study of topological defects in the context of warped space-times. The number of extra dimensions guide us in choosing the right type of defect in order to mimic our brane-world. The key idea for construction of the brane-world is to localize in a very natural way the several fields of our universe (the bosonic ones and fermionic ones). In this way several works have considered five-dimensional universes [2, 3] where five dimensional gravity is coupled to scalar fields. In this scenario, with a specific choice for the scalar potential, it is obtained thin domain wall as solutions that may be interpreted as non-singular versions of the Randall-Sundrum scenario. Besides gravity, the study of localization of fields with several spins it is very important [4]. Also, this type of scenario contributes for discussions about cosmology. In models with 5-dimensional membranes, the mechanism controlling the expansion of the universe have been associated to the thickness of the membrane along the extra dimension [5].

As known, the kind of structure of the considered membrane is very important and will produce implications concerning the methods of field localization. In the works [6, 7] a class of topological defect solutions is constructed starting from a specific deformation of the  $\phi^4$  potential. These new solutions may be used to mimic new brane-worlds containing internal structures [7]. Such internal structures have implications in the density of matter-energy along the extra dimensions [8] and this produces a space-time background whose curvature has a splitting, as we will show, if compared to the usual models. Some characteristics of such model were considered in phase transitions in warped geometries [9].

Motivated by the references above, our main subject here it is to answer the following question: Are these structures able to localize fields of variable spins? In order to find the answer, in this work we propose the analysis of a real scalar field and the gauge tensor field, or Kalb-Ramond field. The paper is organized as follows: in the second section we describe how the deformed membrane is constructed and how the space-time background is obtained; in the third section we study the localization of massless and massive modes of a scalar field in the background obtained; the fourth section treats the behavior of the Kalb-Ramond gauge field by using the same basic steps; the fifth section is important because we introduce the dilaton field in order to force the localization of the Kalb-Ramond field. Such analysis is made in the sixth section. At the final we present our conclusions and perspectives.

## II. TWO-KINK SOLUTIONS MODELING THE BRANE

There is great interest in studying scalar fields coupled to gravity. If we consider a  $D = 5$  universe, we should embed a kink solution in this space-time in order to build our membrane. These kind of solutions are obtained through the

$\lambda\phi^4$  or sine-Gordon potentials. In our case, following the reference [6], we will obtain a new class of defects starting from a deformation of the  $\lambda\phi^4$  potential. In this way we can analyze localization of fields of several ranks in a more complete fashion because the deformed membranes suggests the existence of internal structures. As we will see, this choice avoids space-time singularities also, which is only possible by choosing smooth membrane solutions.

Our model is built with an AdS  $D = 5$  space-time whose metric is given by

$$ds^2 = e^{2A(y)}\eta_{\mu\nu}dx^\mu dx^\nu + dy^2. \quad (1)$$

The warp factor is composed by the function  $A(y)$ , where  $y$  is the extra dimension. The tensor  $\eta_{\mu\nu}$  stands for the Minkowski space-time metric and the indexes  $\mu$  and  $\nu$  go from 0 to 3.

In order to construct the membrane solution we start with an action describing the coupling between a real scalar field and gravitation:

$$S = \int d^5x \sqrt{-G} [2M^3 R - \frac{1}{2}(\partial\phi)^2 - V(\phi)]. \quad (2)$$

In the last action, the field  $\phi$  represents the stuff from which the membrane is made,  $M$  is the Planck constant in  $D = 5$  and  $R$  is the scalar curvature. The equations of motion coming from that action are:

$$\frac{1}{2}(\phi')^2 - V(\phi) = 24M^3(A')^2, \quad (3)$$

and

$$\frac{1}{2}(\phi')^2 + V(\phi) = -12M^3A'' - 24M^3(A')^2. \quad (4)$$

Note that the prime means derivative with respect to the extra dimension. Basically, we look for solutions in which  $\phi$  tends to different values when  $y \rightarrow \pm\infty$ . In a flat space-time we find kink-like solutions for the above equations by choosing a double-well potential. Analogously, if we look for bounce-like solutions in curved space-time, we should regard potentials containing various minima. In the presence of gravity, we can find first order equations by the superpotential method if we take the superpotential  $W(\phi)$  in such a way that  $\frac{\partial W}{\partial\phi} = \phi'$ . Our potential must be defined by

$$V_p(\phi) = \frac{1}{2} \left( \frac{dW}{d\phi} \right)^2 - \frac{8M^3}{3} W^2, \quad (5)$$

from where we can conclude that  $W = -3A'(y)$ . This formalism was initially introduced to study non-supersymmetric domain walls in various dimensions [3, 10].

Following the references [6, 7, 11, 12] the superpotential is given by,

$$W_p(\phi) = \frac{p}{2p-1} \phi^{\frac{2p-1}{p}} - \frac{p}{2p+1} \phi^{\frac{2p+1}{p}}, \quad (6)$$

where  $p$  is an odd integer. The choice for  $W_p$  can be obtained by deforming the usual  $\phi^4$  model and it is introduced in the study of deformed membranes [11]. This choice will permit us to get new and well behaved models for  $p = 1, 3, 5, \dots$  (for  $p = 1$  we get the usual  $\phi^4$  model). For  $p = 3, 5, 7, \dots$ , the potential  $V_p$  has one minimum at  $\phi = 0$  and two at  $\pm 1$ . A new class of solutions called two-kink solutions initially presented in Ref.[7] can be obtained from the choice of the superpotential  $W_p$ . For this we solve  $\frac{\partial W}{\partial\phi} = \phi'$  to find

$$\phi_p(y) = \tanh^p\left(\frac{y}{p}\right). \quad (7)$$

Starting from the first order equation  $W_p = -3A'_p(y)$ , we can find the solution for the function  $A_p(y)$  [11],

$$A_p(y) = -\frac{1}{6} \frac{p}{2p+1} \tanh^{2p}\left(\frac{y}{p}\right) - \frac{1}{3} \left( \frac{p^2}{2p-1} - \frac{p^2}{2p+1} \right) \left\{ \ln \left[ \cosh\left(\frac{y}{p}\right) \right] - \sum_{n=1}^{p-1} \frac{1}{2n} \tanh^{2n}\left(\frac{y}{p}\right) \right\} \quad (8)$$

The function  $A(y)$  determines the behavior of the warp factor. The characteristics of localization for several fields and the construction of effective actions in  $D = 4$  will depend on part of the contribution of the warp factor. Note that the

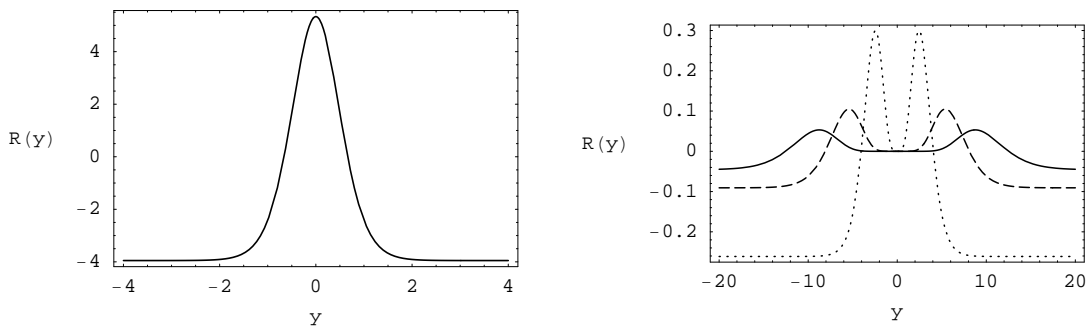


FIG. 1: Plots of the solution of the curvature invariant  $R(y)$   $p = 1$  (left) and for  $p = 3$  (dashed line),  $p = 5$  (dotted line) and  $p = 7$  (solid line) (right) .

exponential factor constructed with this function is localized around the membrane and for large  $y$  it approximates the Randall-Sundrum solution [1]. The solution found here reproduces the Randall-Sundrum model in an specific limit. The space-time now has no singularity because we get a smooth warp factor (because of this, the model is more realistic) [4]. In fact this can be seen by calculating the curvature invariants for this geometry. For example, we obtain

$$R = -[8A_p'' + 20(A_p')^2], \quad (9)$$

Note that the Ricci scalar is finite, which we can observe through the Fig.(1). We can see also an important characteristic of the deformed structure in comparison with the usual thick membrane models generated by simple kinks. Observing again the Fig.(1), for  $p = 1$ , we have the usual curvature scalar for the non-deformed model, the usual one. In this case, the curvature has maximum at  $y = 0$  and goes to negative values when  $y \rightarrow \infty$ . However, regarding the deformed model, taking  $p = 3, 5$  in  $R_p(y)$ , we obtain a splitting with the appearance of a region of zero curvature between two maxima.

### III. SCALAR FIELD

In this section we first analyze the localization of zero-modes for a spin zero (or scalar) field in the background described in the first section. After that we study the spectrum of massive modes for the scalar field in the context of deformed thick brane. It is important to note that our thick brane solution  $\phi_p$  was built from a kink-like solution. We now analyze the localization of the scalar field  $\Phi$  in the membrane described above. We find new aspects for localization on this new background.

#### A. Localized zero-mode

Starting from the membrane discussed in the last section we will analyze the localization of a real scalar field. A similar work can be found in Ref.[13], where a zero mode is studied in a more basic scenario. The deformation give us more details, especially towards the study of field localization. The potential and the wave function are modified when we modify the way the background interacts with the fields of this model. These new solutions show us new behaviors related to resonances and the mass spectrum.

Initially we take the action for the scalar field  $\Phi$  coupled to gravity,

$$\frac{1}{2} \int d^4x dy \sqrt{-G} G^{MN} \partial_M \Phi \partial_N \Phi, \quad (10)$$

where the indexes  $M, N$  go from 0 to 4. We continue by finding the equations of motion,

$$\eta^{\mu\nu} \partial_\mu \partial_\nu \Phi + e^{-2A_p(y)} \partial_y [e^{4A_p(y)} \partial_y \Phi] = 0, \quad (11)$$

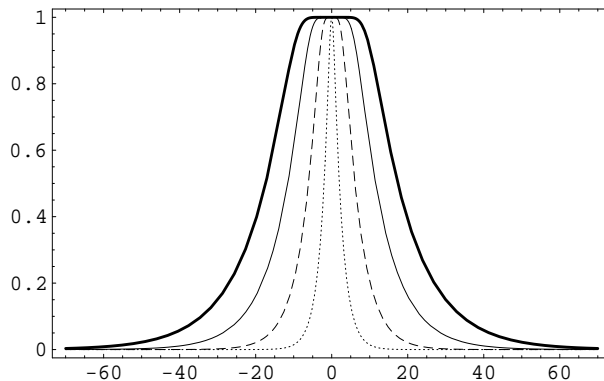


FIG. 2: Plots of  $\psi^2 e^{2A_p}$  for  $p=1$  (points),  $p=3$  (dashed),  $p=5$  (line) and  $p=7$  (thick).

where we have separated the extra dimension from the others. In the next step we use the following separation of variables:

$$\Phi(x, y) = \chi(x)\psi(y). \quad (12)$$

Writing  $\Phi$  as above we arrive at the following equation for the  $y$  dependence:

$$4A'_p \frac{d\psi}{dy} + \frac{d^2\psi}{dy^2} = -m^2 e^{-2A_p} \psi. \quad (13)$$

This equation is very similar to the equation for gravity localization [1]. For  $m^2 = 0$  we see that  $\psi(y) = c$  is a solution, where  $c$  is constant. The condition to obtain a localized scalar zero mode from equation (13) in this case is just to find a behavior which can be interpreted as something trapped to the membrane. In some sense, the solution  $\psi(y) = c$  can not be localized because it is not suppressed in regions far from the membrane. However, the correct way to see localization is by studying the effective action in  $D = 4$ . Going back to the action (10) we make again the procedure of separation of variables and, from the relation (12) and from the result  $\psi(y) = c$ , we get

$$\frac{1}{2} \int_{-\infty}^{+\infty} dy \psi^2 e^{2A_p} \int d^4x \eta^{\mu\nu} \partial_\mu \chi \partial_\nu \chi. \quad (14)$$

The part dependent on the extra dimension in the action above will be determined by the warp factor behavior resulting from this new kind of membrane.

We can observe in Fig.(2) the behavior of the functions important to localization of the effective action (14). We make a plot for several cases of  $A_p$ ,  $p = 1, 3, 5, 7$ . From a first view, it seems that there are good conditions to obtain localization. However, is this result valid for all values of  $p$ ? From Fig.(2), the integral increases if we increase  $p$ . If we demonstrate the convergence of the effective action for every  $p$ , we demonstrate the existence of a localized zero mode for any function  $A_p$ .

In Fig.(3) we compute the evolution of values for the part of the effective action in the extra dimension in terms of  $p$ . The conclusion is that, given a solution for  $\psi(y)$ , for finite values of  $p$ , the warp factor obtained give us localization on the membrane. When  $p \rightarrow \infty$  the warp factor delocalize the zero mode. A similar feature occurs in the study of splitting of thick branes due to phase transitions [9]. In this case, the splitting delocalize the gravitational zero mode.

## B. Massive spectrum

In order to study the Kaluza-Klein states of the scalar field we should rewrite its equation of motion (the part due to the extra dimension) in a Schrodinger-like equation. For this, we get Eq. (13), i. e.,

$$\left\{ \frac{d^2}{dy^2} + 4A'_p \frac{d}{dy} \right\} \psi = -m^2 e^{-2A_p} \psi. \quad (15)$$

and make the following transformation,

$$y \rightarrow z = f(y), \quad \psi = \Omega \bar{\psi}. \quad (16)$$

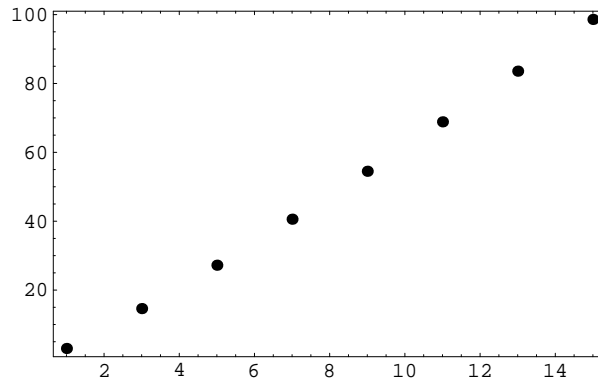


FIG. 3: Plots of  $\int_{-\infty}^{\infty} \psi^2 e^{2A_p} dy$  for various  $p$ .

The conditions to arrive in a Schrodinger-like equation tell us the form of the function  $\Omega$ . In this way we discard terms of first order in derivatives and the right hand side of this equation contains the squared mass  $m^2$ . Then we obtain

$$\Omega = e^{-\frac{3}{2}A}, \quad \frac{dz}{dy} = e^{-A}. \quad (17)$$

Using the transformations (16) the Schrodinger equation can be written as,

$$\left\{ -\frac{d^2}{dz^2} + \bar{V}_p(z) \right\} \bar{\psi} = m^2 \bar{\psi}, \quad (18)$$

where the potential  $\bar{V}_p(z)$  assumes the form

$$\bar{V}_p(z) = e^{2A_p} \left[ \frac{15}{4}(A'_p)^2 + \frac{3}{2}A''_p \right]. \quad (19)$$

We can write the potential in terms of derivatives of the  $z$  variable, i. e.,

$$\bar{V}_p(z) = \left[ \frac{9}{4}(\dot{A}_p)^2 + \frac{3}{2}\ddot{A}_p \right] \quad (20)$$

We plot the potential in Fig.(4) for  $p = 3, 5$  e  $7$ . The figure strongly suggests the presence of resonances in the massive spectra. Obviously, for  $p = 1$  we reobtain the structures of the volcano potential. More interesting details occurs when  $p = 3, 5, 7, \dots$  and we can clearly observe the presence of internal structures [11]. More specifically, for  $p = 1$  we have only one minimum at  $z = 0$ . By changing the values of  $p$ , the potential presents two minima and this is interpreted as the appearance of internal structures. Following Campos [9] reasoning about the potential in the Schrodinger equation in the transverse and traceless sector of metric fluctuations, the appearance of these characteristics are due to a phase transition.

The asymptotical behavior of the potential give us information about the presence of gaps in the spectrum. As we can observe,  $\bar{V}_p(z) \rightarrow 0$  when  $z \rightarrow \infty$ . This excludes the possibility of gaps. Is easy to note that the Schrodinger equation (18) may be written in a supersymmetric quantum mechanical form:

$$Q^\dagger Q \bar{\psi}(z) = \left\{ -\frac{d}{dz} - \frac{3}{2}\dot{A}_p \right\} \left\{ \frac{d}{dz} - \frac{3}{2}\dot{A}_p \right\} \bar{\psi}(z) = m^2 \bar{\psi}(z). \quad (21)$$

In this way we can avoid the existence of tachyonic modes, a necessary condition to keep the stability of the gravitational background discussed here.

As is pointed out in Refs. [2] and [14], for highly massive modes in relation to  $\bar{V}(z)_{max}$ , the potential represents only a little perturbation. Nevertheless, it is possible that modes of the function  $\bar{U}(z)$  for which  $m^2 \leq \bar{V}(z)_{max}$  can resonate with the potential. In order to investigate this possibility it is important to study the wave function  $\bar{\psi}$ , for several eigenvalues  $m^2$ , from the equation (18). We can solve numerically this equation in order to better understand the presence of resonances.

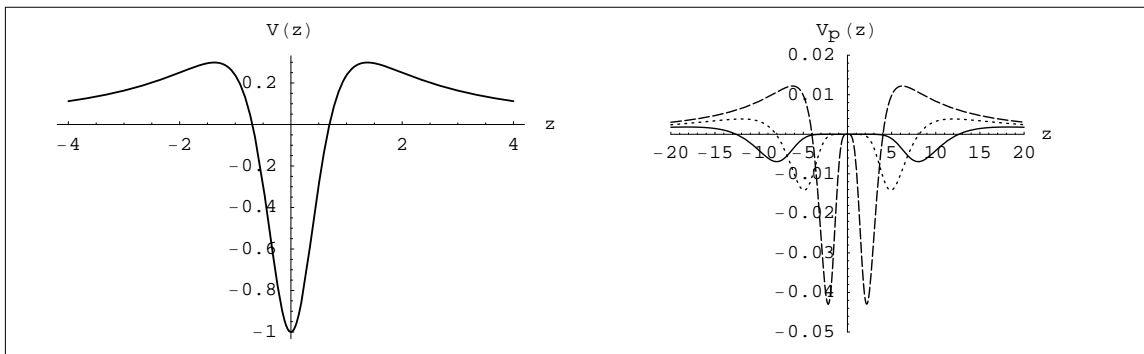


FIG. 4: Plots of  $\overline{V}_p(z)$  for  $p = 1$  (left) and for  $p = 3$  (dashed line),  $p = 5$  (dotted line) and  $p = 7$  (solid line) (right) .

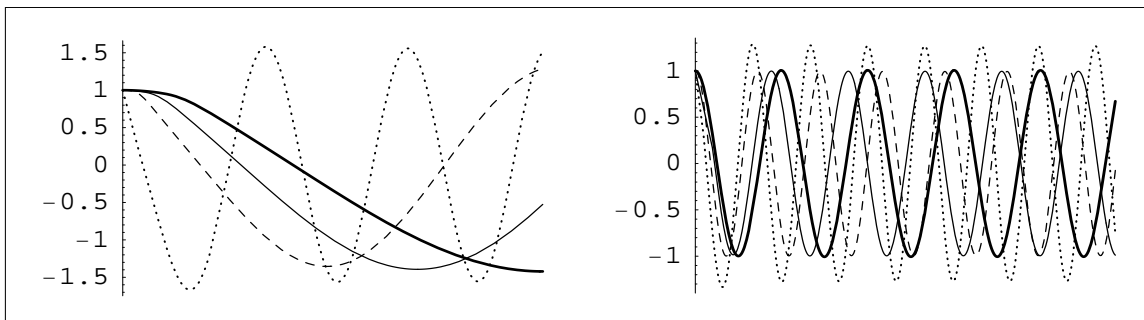


FIG. 5: Plots of  $\overline{V}_p(z)$  for  $p = 1$  (dotted line),  $p = 3$  (dashed line),  $p = 5$  (solid line) and  $p = 7$  (thick line), where we put  $m^2 \leq \overline{V}_p(z)_{max}$  (left) and  $m^2 > \overline{V}_p(z)_{max}$  (right)

Given the potential we should observe the appearance of resonances when  $m^2 \leq \overline{V}_p(z)_{max}$ . The principal signal is that inside the membrane the resonances must have huge amplitude oscillations. With the function  $A_p$  and the potential we plot in Fig.(5) several solutions of the equation (18) for some values of  $m^2$  e  $p$ . As we can see, the wave function oscillates quickly for a moderate value of  $m^2$  and it reduces its period for small values of  $m^2$ . Studying the solutions for the wave function we have not found any evidence of resonances. As mentioned in reference [11], the behavior of the wave function suggests freedom on the bulk without trapping on the membrane.

In order to enlarge our understanding about the coupling between the zero modes and matter inside the membrane we go back to the equation (21). The quantity  $|\chi\overline{\psi}_p(z)|^2$  may be interpreted as the probability of finding the mode in the position  $z$ , where  $\chi$  is a normalization constant [15, 16]. In this way, by computing  $|\chi\overline{\psi}_p(0)|^2$  we will know the probability to find the mode in the membrane. For this, we solve numerically Eq.(18) again, from where we just extract the values  $\overline{\psi}_p(0)$  as functions of the mass. We have limited ourselves to find solutions of Eq.(18) satisfying  $0 < m < 1$  because if  $m^2 \gg V_{max}$  the potential will only represents a small perturbation [2]. In order to normalize the plane wave function we have limited the solutions for each mode to the region  $-100 < z < 100$  and have extracted a normalization constant  $\chi$  for each mass value. With these results at hand we construct the function  $N_p(m) = |\chi\overline{\psi}_p(m)|^2$  which give us the probability of finding the modes at  $z = 0$  as function of  $m$  for each solution  $A_p(z)$  and  $\overline{\psi}_p$ . In the Fig.(6) we plot the function  $N_p(m)$  and observe, for  $p = 1$ , a peak of resonance for  $m = 0$ . This structure is similar to that obtained in Ref.[16] in the study of graviton massive modes. The resonance for  $m = 0$  is consistent with the results presented in section 3.1 where we have obtained, via effective action, a localized zero mode for  $p = 1$ . Considering the Schrodinger equation (18), the coupling of the modes with the matter on the membrane is related to the amplitude of the plane wave function normalized at  $z = 0$  [2]. In our case, we attribute this relation to the value of the function  $N_p(m)$ . The resonance for  $p = 1$  show us that the massive modes do couple weakly with the membrane in comparison with the zero mode. However, observing the solutions of  $N_p(m)$  for  $p = 3, 5, 7$  again in Fig.(6) we verify that the resonant structure for  $m = 0$  tends to disappear when we increase the values for  $p$ . This is related to the fact that we can only guarantee the existence of a zero mode for finite values of  $p$ .

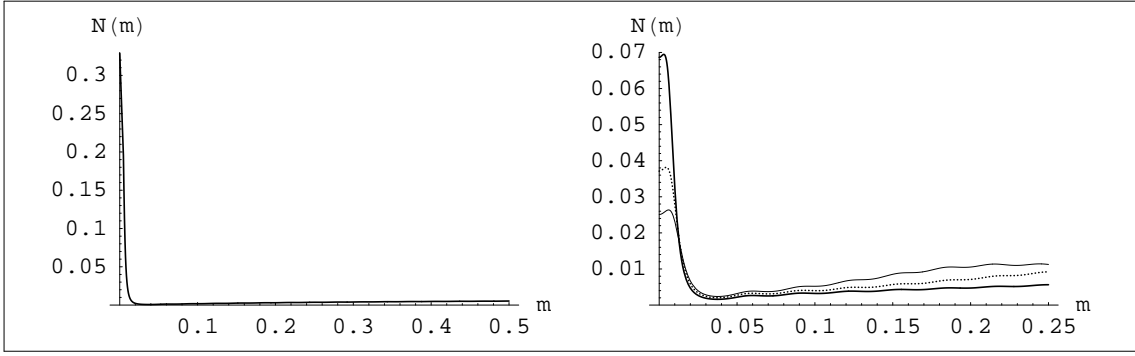


FIG. 6: Plots of  $N_p(m)$  for  $p = 1$  (left),  $p = 3$  (thick line),  $p = 5$  (points) and  $p = 7$  (thin line) (right).

#### IV. THE KALB-RAMOND FIELD

In this section we analyze the behavior of the Kalb-Ramond field in the presence of membranes with internal structures. In this case we study mechanisms of localization and normalization for its zero modes and for their Kaluza-Klein modes.

##### A. Zero-mode

Firstly we introduce in the action of the deformed membrane the Kalb-Ramond field in the following way

$$\int d^5x \sqrt{-G} [2M^3 R - \frac{1}{2}(\partial\phi_p)^2 - V_p(\phi) - H_{MNL}H^{MNL}], \quad (22)$$

where  $H_{MNL} = \partial_{[M}B_{NL]}$  is the field strength for the Kalb-Ramond field. We will make the gauge choice  $B_{\alpha 5} = 0$  in such that its non null components are only those living in the membrane. We have found the equations of motion for  $B_{MN}$  and made explicit the part dependent on the extra dimension:

$$e^{-2A_p} \partial_\mu H^{\mu\gamma\theta} - \partial_y H^{y\gamma\theta} = 0. \quad (23)$$

We make now a separation of variables in order to work the part of the extra dimension,

$$B^{\mu\nu}(x^\alpha, y) = b^{\mu\nu}(x^\alpha)U(y) = b^{\mu\nu}(0)e^{ip_\alpha x^\alpha} U(y), \quad (24)$$

where  $p^2 = -m^2$ . We write  $H^{MNL}$  as  $h^{\mu\nu\lambda}U(y)$ . The equation of motion becomes:

$$\partial_\mu h^{\mu\nu\lambda}U(y) - e^{2A_p} \frac{d^2U(y)}{dy^2} b^{\nu\lambda} e^{ip_\alpha x^\alpha} = 0. \quad (25)$$

The function  $U(y)$  carry all information about the extra dimension and obeys the following equation:

$$\frac{d^2U(y)}{dy^2} = -m^2 e^{-2A_p(y)} U(y) \quad (26)$$

When  $m^2 = 0$  we have the solutions  $U(y) = cy + d$  and  $U(y) = c$  with  $c$  and  $d$  constants. With these at hand we start to make computations in order to find localized zero modes of the Kalb-Ramond field in the deformed membrane. We take the effective action for the tensor field where we decomposed the part dependent on the extra dimension,

$$S \sim \int d^5x \sqrt{-G} (H_{MNL}H^{MNL}) = \int dy U(y)^2 e^{-2A_p(y)} \int d^4x (h_{\mu\nu\lambda}h^{\mu\nu\lambda}). \quad (27)$$

Given the solutions for  $A_p$  and for  $U(y)$  obtained above, we clearly observe that due to the minus sign in the warp factor, the function  $U(y)^2 e^{-2A_p(y)}$  goes to infinity for the two solutions of  $U(y)$ . In this way, the effective action for the zero mode of the Kalb-Ramond field is not finite after integrating the extra dimension.

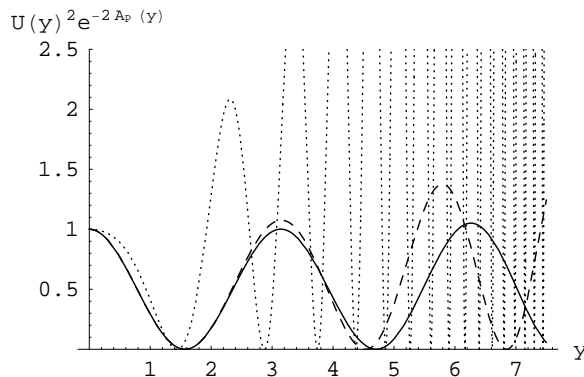


FIG. 7: Plots of  $U(y)^2 e^{-2A_p(y)}$  for  $p = 1$  (dotted line),  $p = 3$  (dashed line) and  $p = 5$  (solid line), where we put  $m = 2$ .

### B. Massive modes

In order to make more complete our analysis of the behavior of the tensor gauge field in this background we can take solutions for  $m \neq 0$  in the equation (26). We must make the following transformation,

$$y \rightarrow z = f(y), \quad f'(y) = e^{-A_p} \quad U(y) = e^{\frac{1}{2}A_p} \bar{U}(z). \quad (28)$$

From where we obtain the equation,

$$\left\{ \frac{d^2}{dz^2} + \bar{V}_p(z) \right\} \bar{U}(z) = -m^2 \bar{\psi}, \quad (29)$$

where

$$\bar{V}_p(z) = e^{2A_p} \left[ \frac{1}{4}(A'_p)^2 + \frac{1}{2}(A''_p) \right]. \quad (30)$$

We can not write the equation above in a supersymmetric form. Then we can not exclude the existence of tachyonic modes. On the other hand, we can find a numerical solution for the function  $\bar{U}(y)$  in the equation (26). In this way we can analyze the details of this solution and its contribution in the effective action for the massive modes of the tensor gauge field. The function  $\bar{U}(y)^2 e^{-2A_p(y)}$ , which is important in the effective action (27), it is plotted in Fig.(7). We can conclude that the effective action is not finite. Therefore, there is no localized massive mode for the Kalb-Ramond field.

### V. DILATONIC DEFORMED BRANE

In the last section, we have not found signals of existence of zero modes or massive modes trapped to the deformed membrane. The coupling between the membrane (described by a two-bounce solution) and the tensor gauge field is strictly due to the space-time metric. Then, if we want to find localized modes we must modify the structure of our membrane.

In this point, we would like following the procedure of Refs.[4, 17], where the gauge field localization is produced by including a new scalar field in the model: the dilaton. By adding this field in the Einstein equations, we obtain a new metric behavior and new information about the dynamics of the membrane. The question here is to understand the behavior of the Kalb-Ramond field in this new background.

The first step in this analysis is to study the Einstein equations in this background. We get the action for the membrane, now with two scalar fields [4],

$$S = \int d^5x \sqrt{-G} [2M^3 R - \frac{1}{2}(\partial\phi)^2 - \frac{1}{2}(\partial\pi)^2 - V_p(\phi, \pi)] \quad (31)$$

where we denote by  $\phi$  the scalar field responsible for the membrane. The field  $\pi$  represents the dilaton. It is assumed a new ansatz for the spacetime metric:

$$ds^2 = e^{2A(y)} \eta_{\mu\nu} dx^\mu dx^\nu + e^{2B(y)} dy^2. \quad (32)$$



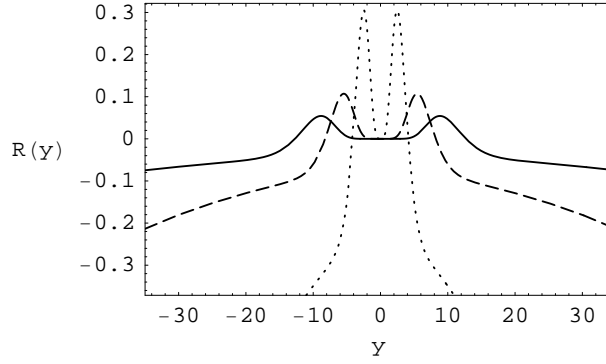


FIG. 8: Plots of the solution of the curvature invariant  $R(y)$  with  $p = 3$  (dotted line),  $p = 5$  (dashed line) and  $p = 7$  (solid line).

The equations of motion are given by

$$\frac{1}{2}(\phi')^2 + \frac{1}{2}(\pi')^2 - e^{2B(y)}V(\phi, \pi) = 24M^3(A')^2, \quad (33)$$

$$\frac{1}{2}(\phi')^2 + \frac{1}{2}(\pi')^2 + e^{2B(y)}V(\phi, \pi) = -12M^3A'' - 24M^3(A')^2 + 12M^3A'B', \quad (34)$$

$$\phi'' + (4A' - B')\phi' = \partial_\phi V, \quad (35)$$

and

$$\pi'' + (4A' - B')\pi' = \partial_\pi V. \quad (36)$$

To obtain the first order equations, we choose the following superpotential  $W_p(\phi)$  [4]:

$$V_p = e^{\frac{\pi}{\sqrt{12M^3}}} \left\{ \frac{1}{2} \left( \frac{\partial W_p}{\partial \phi} \right)^2 - \frac{5M^2}{2} W_p(\phi)^2 \right\}. \quad (37)$$

The two kink solutions of the general form (7) are used in Eq.(6) and we obtain:

$$\pi = -\sqrt{3M^3}A_p, \quad (38)$$

$$B = \frac{A_p}{4} = -\frac{\pi}{4\sqrt{3M^3}}, \quad (39)$$

and

$$A'_p = -\frac{W_p}{3}. \quad (40)$$

Unfortunately, as we can see in Eq.(38), the solution for the dilaton makes the space-time singular. The Ricci scalar for this new geometry is now given by

$$R = -[8A_p'' + 18(A_p')^2]e^{\frac{\pi}{2\sqrt{3M^3}}} \quad (41)$$

From the Fig.(8), there is a region near the membrane where the Ricci scalar is null. When we take different values for  $p$ , the width of this region increases due to the deformation introduced. By another hand, because we have put the dilaton, the curvature scalar decreases indefinitely in regions far from the membrane.

## VI. KALB-RAMOND FIELD ON DILATONIC DEFORMED BRANE

Now we try again to localize the tensor gauge field, but in the new background described in the section above. The issue here is to verify if the dilaton coupling will be enough to localize the Kalb-Ramond field in the deformed membrane. The dilaton coupling is introduced in the model in the following way [18, 19]:

$$S \sim \int d^5x (e^{-\lambda\pi} H_{MNL} H^{MNL}). \quad (42)$$

Therefore, we must analyze the equations of motion of the tensor gauge field in the dilaton background. The new equation of motion is:

$$\partial_M (\sqrt{-g} g^{MP} g^{NQ} g^{LR} e^{-\lambda\pi} H_{PQR}) = 0. \quad (43)$$

With the gauge choice  $B_{\alpha 5} = \partial_\mu B^{\mu\nu} = 0$  and with the separation of variables  $B^{\mu\nu}(x^\alpha, y) = b^{\mu\nu}(x^\alpha)U(y) = b^{\mu\nu}(0)e^{ip_\alpha x^\alpha}U(y)$  where  $p^2 = -m^2$ , it is obtained a differential equation which give us information about the extra dimension, namely

$$\frac{d^2 U(y)}{dy^2} - (\lambda\pi'(y) + B'(y)) \frac{dU(y)}{dy} = -m^2 e^{2(B(y)-A(y))} U(y) \quad (44)$$

For the zero mode,  $m = 0$ , a particular solution of the equation above is simply  $U(y) \equiv cte$ . This is enough for the following discussion. The effective action for the zero mode in  $D = 5$  is

$$S \sim \int d^5x (e^{-\lambda\pi} H_{MNL} H^{MNL}) = \int dy U(y)^2 e^{(-2A(y)+B(y)-\lambda\pi(y))} \int d^4x (h_{\mu\nu\alpha} h^{\mu\nu\alpha}). \quad (45)$$

Given the solution  $U(y)$  constant and regarding the solutions for  $A_p(y)$ ,  $B(y)$  e  $\pi(y)$ , it is possible to show clearly that the integral in the  $y$  variable above is finite if  $\lambda > \frac{7}{4\sqrt{3M^3}}$ , and for  $p$  finite. As a consequence, for a specific value of the coupling constant  $\lambda$  it is possible to obtain a localized zero mode of the Kalb-Ramond field.

We should now consider a discussion about massive modes in this background. For this, we must analyze the Eq. (44) for  $m \neq 0$  trying to write it in a Schroedinger-like equation through the following change

$$y \rightarrow z = f(y), \quad U = \Omega \bar{U}, \quad (46)$$

with

$$\Omega = e^{(\frac{\alpha}{2} + \frac{3}{8})A}, \quad \frac{dz}{dy} = e^{-\frac{3}{4}A}, \quad (47)$$

were,

$$\alpha = \frac{1}{4} - \sqrt{3M^3}\lambda. \quad (48)$$

After all the necessary calculations we arrive at the equation we want to analyze, namely

$$\left\{ -\frac{d^2}{dz^2} + \bar{V}(z) \right\} \bar{U} = m^2 \bar{U}, \quad (49)$$

where the potential  $\bar{V}_p(z)$  assumes the form,

$$\bar{V}(z) = e^{\frac{3}{2}A} \left[ \left( \frac{\alpha^2}{4} - \frac{9}{64} \right) (A')^2 - \left( \frac{\alpha}{2} + \frac{3}{8} \right) A'' \right]. \quad (50)$$

We can write the potential in function of the derivatives respect to  $z$ ,

$$\bar{V}_p(z) = \left[ \beta^2 (\dot{A}_p)^2 - \beta \ddot{A}_p \right], \quad (51)$$

where,

$$\beta = \frac{\alpha}{2} + \frac{3}{8}. \quad (52)$$

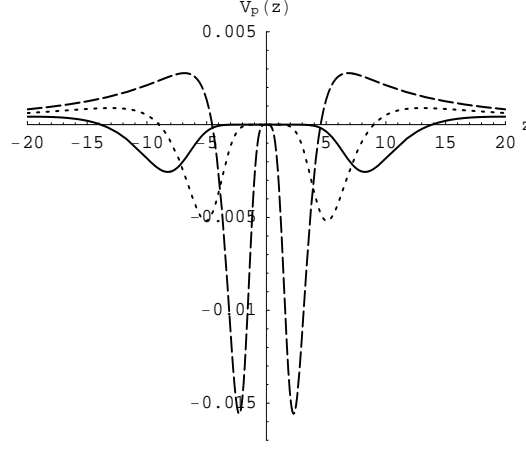


FIG. 9: Plots of the potential  $\bar{V}_p(z)$  with  $p = 3$  (dashed line),  $p = 5$  (dotted line) and  $p = 7$  (solid line). We have put  $\sqrt{3M^3}\lambda = 2$ .

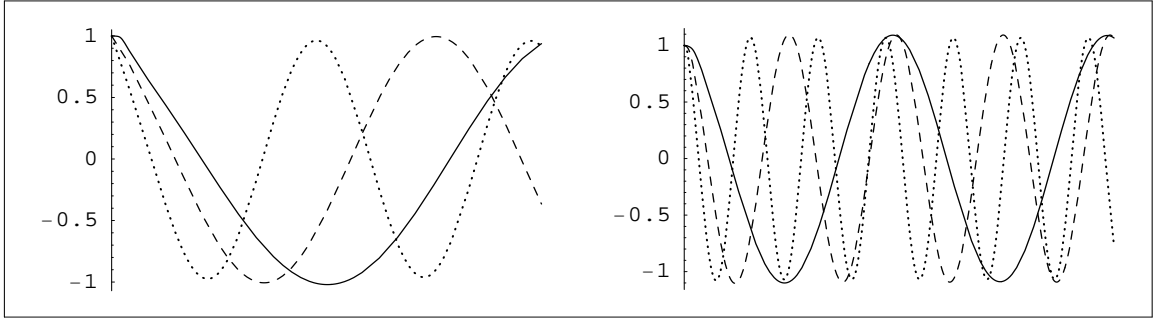


FIG. 10: Plots of  $\bar{U}_p(z)$  for  $p = 1$  (dotted line),  $p = 3$  (dashed line),  $p = 5$  (solid line) and  $p = 7$  (thick line), where we put  $m^2 \leq \bar{V}_p(z)_{max}$  (left) and  $m^2 > \bar{V}_p(z)_{max}$  (right)

We can see from the Fig.(9) that the potential is affected by the deformation procedure introduced in this work. We identify the existence of two minima whose distance increases when we increase the values of  $p$ . The form of the potential is also directly changed. Note that we use  $\sqrt{3M^3}\lambda > 1$  in order to obtain a potential like (51), i.e., the standard form found when we write Schrodinger-like equations. This choice is fundamental in order to find finite results regarding the behavior of the Kalb-Ramond field.

It is interesting to point out that the Schrodinger-type equation (49) can be written in the supersymmetric quantum mechanics scenario as follows,

$$Q^\dagger Q \bar{U}(z) = \left\{ \frac{d}{dz} - \beta \dot{A} \right\} \left\{ \frac{d}{dz} + \beta \dot{A} \right\} \bar{U}(z) = -m^2 \bar{U}(z). \quad (53)$$

From the form of the Eq. (53), we exclude the possibility of normalized negative energy modes to exist. On the other hand, we exclude also the possibility of the presence of tachyonic modes, which is a necessary condition to keep the stability of gravitational background.

We cannot find analytical solution of the massive modes wave function in Schrodinger equation. However we will be able to analyze the solution for  $\bar{U}_p$  by numerically solving the equation (49). We plot in Fig.(10) the wave function so obtained for two values of  $m^2$ . As we can observe, when we make  $m^2 > \bar{V}_p(z)_{max}$ , we minimize the contribution due to the deformations over the solution  $\bar{U}_p$ . However, regarding  $m^2 \leq \bar{V}_p(z)_{max}$ , as we increase  $p$  we reduce the frequency of oscillations of the solutions  $\bar{U}_p$ . We must remember that the search for finite solutions it was only possible due to the choice  $\sqrt{3M^3}\lambda > 1$ .

As mentioned in Ref. [11], the behavior of the wave function suggests us a free motion in the bulk, but no trapping in the membrane.

An interesting point to be investigated is how the intensity of the dilaton constant coupling may modify the patterns of solutions observed in Fig.(10). For this, we solve again the equation (49), but this time, changing the values of the

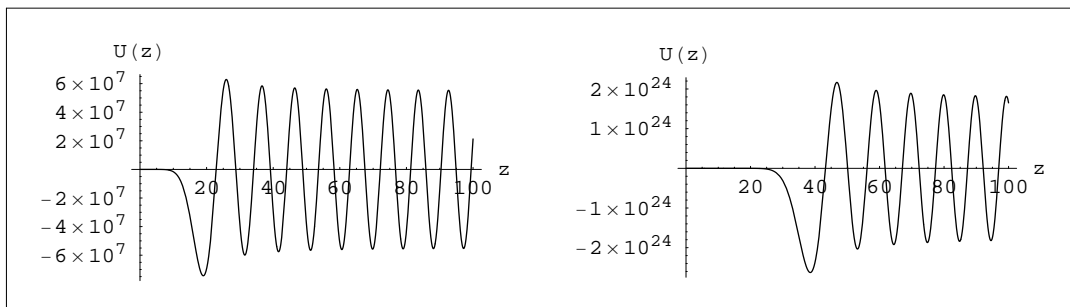


FIG. 11: Plots of  $\overline{U}_p(z)$  for  $p = 1$ , where we put  $m = 0, 5$ ,  $\sqrt{3M^3\lambda} = 20$  (left) and  $\sqrt{3M^3\lambda} = 40$  (right)

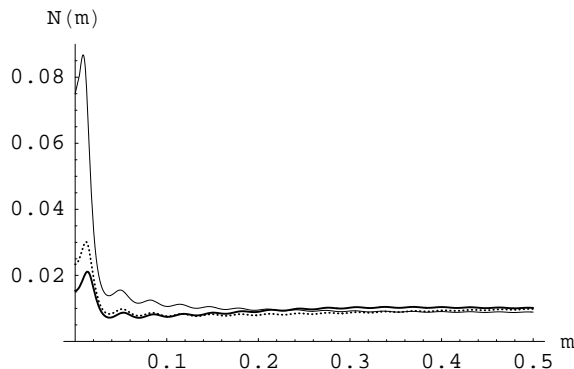


FIG. 12: Plots of  $M_p(m)$  for  $p = 1$  (thin line),  $p = 3$  (points) and  $p = 5$  (thick line).

constant coupling  $\lambda$ . We plot in Fig.(11) the function  $\overline{U}_p(z)$ , this time for  $\sqrt{3M^3\lambda} = 20$  on the left and  $\sqrt{3M^3\lambda} = 40$  on the right. We note the suppression of the mode oscillations in regions near the membrane due to the increasing of  $\lambda$ . On the other hand, in regions far away from  $z = 0$  the amplitude oscillations grows.

In order to better understand the coupling between massive modes and matter on the membrane we should know, starting from Eq.(53), the amplitude of the plane wave function  $\overline{U}_p(z)$  normalized at  $z = 0$ . The quantity  $|\zeta\overline{U}_p(0)|^2$ , being  $\zeta$  a normalization constant, should give us the probability of finding a mode of mass  $m$  at  $z = 0$ . In the Fig.(12) we plot  $M_p(m) = |\zeta\overline{U}_p(0)|^2$  where we can identify, for  $p = 1$ , a resonant peak near  $m = 0$ , precisely for  $m = 9 \times 10^{-3}$ . We may interpret that, in this case, the probability of finding light modes or massless modes coupled to the membrane is bigger than for heavier modes. This characteristics disappears when we change the values of  $p$ . As we can observe in Fig.(12), the resonant structure tends to disappear in accordance to the results of localization of the zero mode. We can still test the consistency of the above results regarding again the model without the dilaton coupling, sections 4.1 and 4.2. In this case, we do not find signals of localization of the Kalb-Ramond field. In this way, we can extract the function  $M_p(m)$  from equation (29) by the same steps discussed before and plot the results in Fig.(13). As we expect, the resonant structure disappears and the couplings of the zero modes is highly suppressed.

## VII. CONCLUSIONS

In this article we analyze under several aspects the localization properties of a real scalar field and the Kalb-Ramond tensor gauge field in a very specific type of membrane: the deformed membrane.

We have obtained a scalar zero mode whose existence obeys to a restriction due to the deformation structure included in the analysis. When we consider massive modes, we obtain through a Schrodinger-like equation an effective potential different of that found in the usual models of membranes of the kink type. In the spectrum of massive states we have found a resonance near the membrane through the probability function. This resonance disappears when we deform more and more the membrane, i.e., we increase the number  $p$  in the membrane solutions. In general, we can conclude that the zero mode coupling to the membrane is bigger than the massive mode coupling one.

The analysis of the Kalb-Ramond field it is jeopardized since the effective action is not normalizable: we have

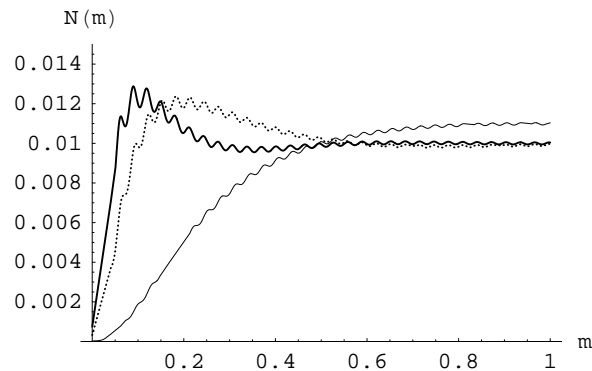


FIG. 13: Plots of  $M_p(m)$  for  $p = 1$  (thin line),  $p = 3$  (points) and  $p = 5$  (thick line).

not zero modes for the Kalb-Ramond field. The resulting equation of motion for the massive modes is not found and it can not be written in a form of Schrodinger-like equation. This fact do not allows us to interpret quantum mechanically the problem. What we do to circumvent this result is to add one more field in the model, the dilaton, and this changes a little the gravitational background. After this modification, we can, under some conditions, find a localized tensorial zero mode. Related to the spectra of massive states, we see that the effective potential in the Schrodinger-like equation is affected by the deformations made in the membranes. The numerical analysis of that equation for massive states reveals that there are plane waves describing the free propagation of particles in the bulk. The dilaton coupling change the amplitude of oscillations of the modes away from the membrane. Indeed, studying the coupling of the matter massive states with the membrane we have found a resonance, which again disappears with the deformations. The resonance structures show us that only light modes of the KK spectrum present not suppressed coupling with the membrane. Finally, we showed the consistency of the results obtained with those from the model without the dilaton.

The authors would like to thank Fundação Cearense de apoio ao Desenvolvimento Científico e Tecnológico (FUNCAP) and Conselho Nacional de Desenvolvimento Científico e Tecnológico (CNPq) for financial support.

- 
- [1] L. Randall, R. Sundrum, Phys. Rev. Lett. 83, 3370 (1999); *ibid* 83, 4690 (1999).
  - [2] M. Gremm, Phys. Lett. B478, 434 (2000).
  - [3] O. Dewolfe, D.Z. Freedman, S.S. Gubser, and A. Karch, Phys. Rev. D **62**, 046008 (2000).
  - [4] A. Kehagias, K. Tamvakis, *Localized gravitons, gauge bosons and chiral fermions in smooth spaces generated by a bounce*, Phys. Lett. B504, 38 (2001).
  - [5] M. Sadegh Movahed and Sima Ghassemi, Phys. Rev. D **76**, 084037 (2007)
  - [6] D. Bazeia, L. Losano, Phys. Rev. **D73**, 025016 (2006).
  - [7] D. Bazeia, J. Menezes, and R. Menezes, Phys. Rev. Lett. 91, 241601 (2003)
  - [8] D. Bazeia, C. Furtado, A.R. Gomes, JCAP **0402** 002, (2004)
  - [9] A. Campos, Phys. Rev. Lett. **88**, 141602 (2002).
  - [10] K. Skenderis, P.K. Townsend, Phys. Lett. B**468**, 46 (1999).
  - [11] D. Bazeia, A.R. Gomes, JHEP **0405**, 012 (2004).
  - [12] D. Bazeia, R. F. Ribeiro, M. M. Santos, Phys. Rev. D**54**, 1852 (1996).
  - [13] Borut Bajc, Gregory Gabadadze, Phys. Lett. B**474**, 282-291, (2000).
  - [14] C. Csaki, J. Erlich, T. J. Hollowood, Y. Shirman, Nucl. Phys. B**581**, 309 (2000).
  - [15] C. A. S. Almeida , M. M. Ferreira, Jr. , A. R. Gomes , R. Casana, *Fermion localization and resonances on two-field thick branes*, hep-th/09013543. To appear in Physical Review D.
  - [16] C. Csaki, J. Erlich, T. J. Hollowood, Y. Shirman, Phys. Rev. Lett. 84, 5932-5935 (2000).
  - [17] Kazuo Ghoroku, Motoi Tachibana, Nobuhiro Uekusa, Phys. Rev. D**68**, 125002 (2003).
  - [18] K. Sfetsos and A. A. Tseytlin, Phys. Rev. D**49**, 2933 (1994).
  - [19] B. Kleihaus, J. Kunz, K. Myklevoll, Phys. Lett. B**605**, 151 (2005).